

# UC Irvine

## UC Irvine Previously Published Works

### Title

The transport of test ions in a quiet plasma

### Permalink

<https://escholarship.org/uc/item/5sp9t6np>

### Journal

The Physics of Fluids, 30(9)

### ISSN

0031-9171

### Authors

McWilliams, Roger

Okubo, Mason

### Publication Date

1987-09-01

### DOI

10.1063/1.866510

### Copyright Information

This work is made available under the terms of a Creative Commons Attribution License, available at <https://creativecommons.org/licenses/by/4.0/>

Peer reviewed

# The transport of test ions in a quiet plasma

Roger McWilliams and Mason Okubo

*Department of Physics, University of California, Irvine, California 92717*

(Received 30 March 1987; accepted 11 June 1987)

Experimental measurements of cross-field transport of test ions in a quiet plasma are reported. In a plasma with density fluctuations below  $\langle (\delta n/n_0)^2 \rangle^{1/2} \approx 0.002$ , the experimental results agree with simple predictions of test ion diffusion resulting from collisional processes for the range of parameters tested. The observed transport may be attributed to Coulomb collisions and the results disagree with predictions based solely on Bohm diffusion or turbulent processes.

## I. INTRODUCTION

The nature of plasmas is such that they can provide an excellent medium for the study of natural phenomena where statistical physics plays a significant role. For example, the understanding of stochastic processes can be advanced by examining plasmas. Considerable experimental and theoretical effort has gone into studying plasma transport resulting from irreversible processes. Underlying much of this work is the notion of the motion of a dressed test particle<sup>1-4</sup> reacting to fluctuating fields. Many theories and experiments concerning diffusion have been developed. Experimentally, most measurements of diffusive processes in plasmas have studied bulk plasma processes. In this paper an experiment is described wherein a method for creating test particles and following their subsequent motion in a plasma was performed.

Experimentally, there has been substantial effort made to understand the underlying processes responsible for transport of particles across magnetic fields. Most experiments have been unable to distinguish one plasma ion from another and hence have measured bulk plasma motion rather than the motion of test particles. Such experiments include those done by D'Angelo and Rynn,<sup>5,6</sup> Stodiek, Ellis, and Gordon,<sup>7</sup> Rynn,<sup>8</sup> D'Angelo,<sup>9</sup> D'Angelo and von Goeler,<sup>10</sup> Motley,<sup>11</sup> Wolf and Rogers,<sup>12</sup> von Goeler and Motley,<sup>13</sup> von Goeler, Sadowski, Pacher, and Yoshikawa,<sup>14</sup> and Guilino.<sup>15</sup> An attempt to measure transport coefficients via injection of a second ion species into a plasma was done by Eastlund,<sup>16</sup> but the results were inconclusive. Test electron and ion beams were injected into a turbulent plasma by Stenzel and Gekelman,<sup>17</sup> with the electron motion exhibiting Bohm scaling. Collisional drift waves with  $\delta n/n \approx 0.1$  were found to cause substantial diffusion by Hendel, Chu, and Politzer.<sup>18</sup> An important advance in the measurement of transport processes is the method of optical tagging to measure test particle transport, demonstrated by Stern, Hill, and Rynn.<sup>19</sup> Experiments using optical tagging which showed anomalous cross-field transport in the presence of sizable wave fluctuations were reported by McWilliams, Hill, Wolf, and Rynn.<sup>20</sup>

A considerable body of transport work has emerged in tokamak research. Neutral beam injection has led to scaling laws such as those developed by Kaye and Goldston.<sup>21</sup> Impurity injection experiments by Marmor<sup>22</sup> and others have led to models of radial transport from empirical observation.

Extensive reviews of neoclassical transport results and theories have been given by Hinton and Hazeltine<sup>23</sup> and Liewer.<sup>24</sup> Many theories have been developed and many empirical observations have been made, but underlying this body of work is a need to make a specific connection between the transport processes and the responsible microturbulent or classical mechanisms.

This paper describes an experiment where the motion of a test ion population could be followed as it moved through a plasma. The turbulence level in the plasma was sufficiently low that transport theories which depend explicitly on turbulence predict that classical diffusion would be the dominant diffusive mechanism. The experimental results for the inferred test ion spatial diffusion coefficient were found to agree with simple classical diffusion predictions over the range of plasma parameters tested.

## II. TEST PARTICLE DIFFUSION THEORY

Consider a plasma where the turbulent wave spectrum is not enhanced by instabilities above the thermal noise level. In simple magnetized and unmagnetized plasmas the electric field fluctuation level was expressed by Rostoker,<sup>1</sup> from which an estimate of the density fluctuation level may be made. For the conditions of the experiment (measured at the center of the plasma column), the density fluctuation level  $\langle (\delta n)^2 \rangle^{1/2}/n_0$  is estimated from the theory to be about  $7 \times 10^{-3}$ , a little above the measured values. At the edge of the plasma column the density fluctuation level was found to be higher than this theoretical estimate and is attributed to drift wave turbulence,<sup>18</sup> where drift waves could be driven by the radial density gradient. Hence all of the experimental measurements were taken near the center of the plasma column where the density fluctuations did not exceed  $2 \times 10^{-3}$  for the quiet plasma measurements. Under these circumstances turbulent diffusion may be expected to be dominated by classical collisional diffusion processes, as shown below.

To develop a model for collisional diffusion of a test particle, one may start with the Langevin equation,

$$\frac{d\mathbf{u}}{dt} = -\beta\mathbf{u} + \mathbf{A}(t), \quad (1)$$

as described by Chandrasekhar.<sup>25</sup> In Eq. (1),  $\mathbf{u}(t)$  is the velocity of the test particle, and the force per unit mass acting on the particle has been divided into a frictional drag term  $-\beta\mathbf{u}$  and a fluctuating part  $\mathbf{A}(t)$ . There are several

assumptions made to obtain the solution to Eq. (1), namely, (i) temporal homogeneity; (ii)  $\mathbf{A}(t)$  is described by a Markov process with a fluctuation time far less than the time for measurable variation in  $\mathbf{u}$ ; and (iii)  $\beta$  is not a function of  $\mathbf{u}$ . For times  $t \gg 1/\beta$ , Eq. (1) led Chandrasekhar to conclude

$$\langle (x - x_0)^2 \rangle_{ave} = \frac{1}{3} \langle |\mathbf{r} - \mathbf{r}_0|^2 \rangle_{ave} = 2Dt = (2T/m\beta)t, \quad (2)$$

where  $D$  is the diffusion coefficient of test particles with mass  $m$ . In determining the application of the Langevin equation to the motion of a test ion in a plasma, one may note there will be an exponentially small class of ions where the Coulomb interaction process will violate the third of these assumptions (since the collision frequency is velocity dependent), but the bulk of the ion population will fit these assumptions. Under conditions fitting Eq. (1), Thompson<sup>26</sup> (among others) has determined the diffusion coefficient. Using Kac's<sup>27</sup> analysis of the Ehrenfest model also shows that the recurrence time for the experimental measurements may be estimated to be in excess of  $10^8$  sec and hence the diffusive process may be viewed as an irreversible process in the plasma.

Considering a plasma in an external magnetic field,  $\mathbf{B} = B\hat{z}$ , causes Eq. (1) to be modified to

$$\frac{d\mathbf{u}}{dt} = -\beta\mathbf{u} + \mathbf{A}(t) + \mathbf{u} \times \omega_c, \quad (3)$$

where  $\omega_c = eB/mc$ . Writing  $\mathbf{u}_+ = u_x + iu_y$ ,  $A_+ = A_x + iA_y$ , and  $\bar{\beta} = \beta + i\omega_c$  and looking for the long-time solution to (3), i.e.,  $t \gg 1/\beta$ ,  $1/\omega_c$ , one obtains

$$\langle (x - x_0)^2 + (y - y_0)^2 \rangle = 2(T/m) [\beta / (\beta^2 + \omega_c^2)] t. \quad (4)$$

For the circumstances  $\beta^2/\omega_c^2 \ll 1$  the diffusion coefficient is given by

$$D_1 = \frac{1}{2} \rho_i^2 \nu_{ii} \quad (5)$$

for a test ion in a quiet plasma with  $T_i \approx T_e$ , where  $\rho_i$  is the Larmor radius and  $\nu_{ii}$  is the collision frequency of the test ions. Note that assumption (iii) was invoked to obtain Eq. (5) through the  $\beta = \beta(v_{ii})$ . It is not readily apparent how the addition of realistic plasma effects which violate parts of the three assumptions will change the prediction of Eq. (5). Hence, Eq. (5) should be taken as a sample theoretical prediction which possibly does not include some physical elements required for a precise description of collisional transport of test ions in a plasma. The result from Eq. (5) is similar to that obtained by Rostoker<sup>1</sup> and Klimontovich.<sup>28</sup>

Like-particle collisions, as well as electron-ion collisions also were considered by Simon,<sup>29</sup> Longmire and Rosenbluth,<sup>30</sup> and Taylor.<sup>31</sup> Like-particle collisions between indistinguishable particles do not lead to diffusion until third order spatial derivatives are included in the flux calculations. An estimate of the flux resulting from third order effects in the experiments predicts a contribution of less than 1% of the flux predicted by Eq. (5). Calculations of electron-ion collisional diffusion show that the test particle diffusion coefficient in Eq. (5) exceeds the ion-electron diffusion coefficient by  $(m_i/m_e)^{1/2}$ , which is much greater than unity.

### III. EXPERIMENT

The experiments were performed in the University of California, Irvine Q-Machine,<sup>32</sup> which was run single ended (see Fig. 1). The nearly completely ionized barium plasma was formed via contact ionization on a rhenium-plated tungsten hot plate. The resulting 5 cm diam plasma flows down the axial magnetic field,  $B_0 = B_0\hat{z}$  with  $B_0 < 7$  kG, typically at a speed of  $5 \times 10^4 < v_z < 1 \times 10^5$  cm/sec, and is buried at a cold floating plate 1.4 m downstream. Initial electron and ion temperatures are approximately 0.2 eV. Electron temperature was inferred from a Langmuir probe while ion velocity distributions were obtained using laser induced fluorescence techniques (to be discussed later). Plasma densities were  $5 \times 10^9 \leq n_e \leq 1.7 \times 10^{10}$  cm<sup>-3</sup>, the density being inferred from Langmuir probes and through the angle of propagation of a lower hybrid test wave ( $\theta \approx \omega/\omega_{pe}$  w.r.t.  $\mathbf{B}_0$ ).<sup>33</sup>

In creating test particles in a plasma it is important to create a test particle population such that test particle-test particle collisions are rare compared to test particle-background plasma collisions. The reason for this is that collisions between indistinguishable particles do not lead to significant diffusion even though the individual particle orbits are affected. In following the diffusive motion of a test particle population it is therefore important to create a test particle population which is only a few percent of the background density so that the measured diffusion coefficient will not be reduced by like-particle collisions.

Laser induced fluorescence (LIF) was used to create and follow the test ions in the experiment (see Fig. 1); the details of LIF are described in Refs. 34-38. The test ion population was created in a manner similar to that reported in Refs. 19 and 20. The LIF diagnostic uses a dye laser, tuned to 5854 Å (broadband in this experiment), to induce transitions from the  $5^2D_{3/2}$  metastable state of singly ionized BaII to the  $6^2P_{3/2}$  excited state. The excited state decays in a few nanoseconds<sup>39</sup> to the  $6^2S_{1/2}$  ground state, emitting fluorescence at 4554 Å, detected with a lens and photomultiplier.

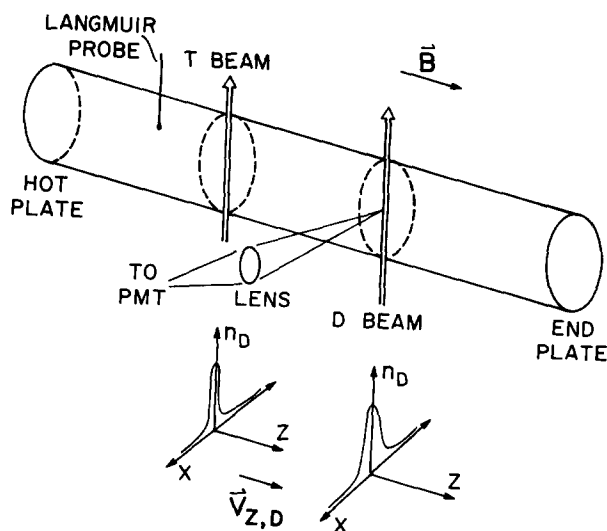


FIG. 1. General plasma configuration and diagnostic geometry. Cylindrical plasma formed at the hot plate drifts down the magnetic field to the end-plate, where it is lost. T and D beams are the tagging and detection laser beams, respectively.

An exact relationship of the fluorescence intensity to the density of excited ions is found by examining the transition rate equations,<sup>40</sup> depends on the metastable population (typically about 8% of the total plasma density), and involves kinetic effects.<sup>38,41</sup> By examining ion velocity distribution functions<sup>42,43</sup> one may conclude that the fluorescence intensity is proportional to the metastable ion density for this experiment.

The cross-field diffusion measurements described in this paper were made using this technique of optical tagging<sup>19,20</sup> in which a population of ions is marked spectroscopically. Running the laser broadband tags the metastable population regardless of ion velocity. As shown in Fig. 1, the plasma ions stream from the hot plate. A small group of them pass through the tag beam (T beam), where the local metastable population is depleted by transitions into ground state induced by the laser. A tagged population of ions, when passing through the detection beam (D beam), signals its presence by a reduction in the induced transitions, indicating an ion flux between tag and detection beams. We refer to this technique as dark-pulse tagging. Signal resolution was enhanced substantially by chopping the tag signal and using synchronous detection. The axial spatial separation of the tagging and detection could be made as small as 1 cm or as large as 20 cm. Measuring the cross-field spatial motion of the tagged ions by the cross-field scanning of the detection beam allowed the test particle transport coefficients to be determined. Clearly this optical tagging technique requires an ion population which can be tagged. Hence many plasmas would require the injection of a taggable ion beam to be able to perform similar transport experiments.

If there are no sources or sinks of metastables other than the hot plate (at which the ions were created) and the laser beam which creates the tagged population, then any mechanisms for cross-field transport will change the spatial distribution of a tagged population drifting axially down the field lines. The density of particles will satisfy the continuity equation

$$\frac{\partial}{\partial t} n_D + \nabla \cdot \Gamma_D = 0, \quad (6)$$

where  $n_D$  is the number density of the tagged particles and  $\Gamma_D$  is the flux of  $n_D$  into (out of) the tag region. If the flux is a result of a bulk motion, then  $\Gamma = n\mathbf{v} = n\langle \mathbf{x} \rangle / \tau$ , where  $\tau$  is the time it takes to shift the average position of a group of particles by  $\langle \mathbf{x} \rangle$ . If the flux is a diffusive flux a simple model may apply, where  $\Gamma = -D\nabla n = -(\langle \mathbf{x}^2 \rangle / \tau) \nabla n$ , and where  $D$  is the diffusion coefficient. There would then be a spreading of the group of particles which satisfies the equation

$$\frac{\partial}{\partial t} n_D - \nabla \cdot (D\nabla n_D) = 0. \quad (7)$$

Ions, drifting along the magnetic field lines, enter the vertical (parallel to the  $y$  axis) tagging laser beam (see Fig. 1) whence they continue on as a laser-beam-shaped population of tagged ions. Diffusive processes described by Eq. (7) and Larmor orbits will cause a horizontal (parallel to the  $x$  axis) spreading of this distribution. By measurement of the width of the fluorescence signal, the diffusive spreading, and thus

the diffusion coefficient, can be determined.

Given an initial distribution  $f(\xi, v_\perp, \phi, t = 0)$  of tagged particles at the horizontal position  $x = \xi$ , with perpendicular (to  $\mathbf{B}_0$ ) velocity component  $v_\perp$  moving in a direction  $\phi$  with respect to the laser beam, it is possible to determine the subsequent time evolution of the distribution and its dependence on any diffusion processes that may be present. Particles tagged at  $x = \xi$  will experience a diffusive motion of their guiding centers, causing a spreading of the distribution.

In addition to these diffusive processes, the thermal distribution of perpendicular velocities (giving a range of Larmor orbit sizes) and the distribution of angles at which the particles can leave the beam will affect the time evolution of the spatial distribution. Figure 2 shows how two particles with different Larmor orbit sizes entering the tag laser beam at different positions ( $\xi_1$  and  $\xi_2$ ), with different phases in their orbits ( $\phi_1$  and  $\phi_2$ ), can give a width to the tagged signal greater than the laser beam width. In the absence of diffusion, a particle tagged at  $x = \xi$  will be found, after a time  $t$ , at

$$x(t) = \xi - v_\perp / \omega_{ci} [\cos \phi - \cos(\omega_{ci}t + \phi)]. \quad (8)$$

The density of particles at  $(x, t)$ , resulting from particles tagged at  $\xi$ , is

$$n_D(x, t; \xi) = \int v_\perp dv_\perp \int d\phi f(\xi, v_\perp, \phi, t) \delta\{x - \xi + v_\perp / \omega_{ci} [\cos \phi - \cos(\omega_{ci}t + \phi)]\}. \quad (9)$$

Since the beam has a finite size, particles from different  $\xi$ , initial tag points, may contribute to the number of particles detected at  $x$ . Summing over these contributions, the density of particles at  $(x, t)$  becomes

$$n_D(x, t) = \int d\xi \int v_\perp dv_\perp \int d\phi f(\xi, v_\perp, \phi, t) \delta\{x - \xi + v_\perp / \omega_{ci} [\cos \phi - \cos(\omega_{ci}t + \phi)]\}. \quad (10)$$

Since the field of the laser mode has a Gaussian radial intensity profile in the plasma, the distribution of tagged particles  $f(\xi, v_\perp, \phi, 0)$  will have a Gaussian spatial dependence. Since the measured velocity space distribution is a Maxwellian,<sup>38,43</sup> for the case of the unperturbed plasma, the distribution of tagged particles will have a Gaussian velocity-space

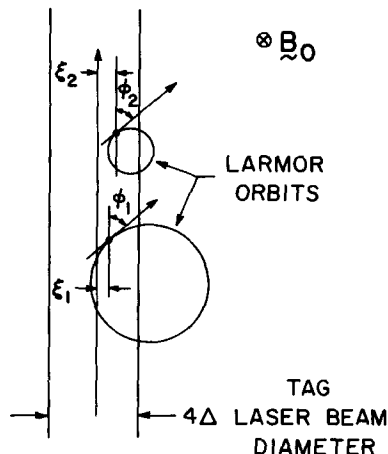


FIG. 2. Phase and position of two different ions as they enter the tagging laser beam.

dependence. Thus  $f(\xi, v_1, \phi, 0)$  becomes

$$f(\xi, v_1, \phi, 0) = N_0 \exp(-\xi^2/4\Delta^2) \exp(-v_1^2/\sigma^2), \quad (11)$$

where  $2\Delta$  is the initial half-width of the distribution in coordinate space and  $\sigma$  is the thermal width of the velocity space distribution.

Since the guiding-center drift evolution of the particle density is governed by the perpendicular component of the diffusion equation [Eq. (7)], the average time development of the spatial distribution can be determined by taking a Laplace and Fourier transform into  $(k, \omega)$  space. The characteristic equation, which can be derived from the transformed diffusion equation, gives a relationship between  $\omega$  and  $k$ ,

$$\omega = -iD_1 k^2, \quad (12)$$

where  $D_1$  is the coefficient of diffusion perpendicular to  $\mathbf{B}_0$ . With Eq. (12) and the Laplace transform of the initial spatial distribution

$$f(k, v_1, \phi, 0) = N_1 \exp(-k^2 \Delta^2), \quad (13)$$

the time-dependent spatial distribution can be derived using the inverse Laplace transform

$$f(\xi, v_1, \phi, t) = \int f(k, v_1, \phi, 0) \exp[-i(k\xi - \omega t)] dk. \quad (14)$$

Solving the integral results in

$$f(\xi, v_1, \phi, t) = N_1 \exp[-\xi^2/(2\Delta^2 + 4D_1 t)]. \quad (15)$$

This is the time-dependent spatial distribution of tag particles including diffusive processes. By substituting  $f(\xi, v_1, \phi, t)$  into Eq. (10) for the total density of particles and changing the delta function from an  $x$ -dependent argument to a  $v_1$ -dependent argument, the integral over  $dv_1$  and  $d\phi$  can be done, resulting in

$$n_D(x, t) = B \int d\xi \exp\left(-\frac{\xi^2}{2\lambda^2}\right) \exp[-\beta(x - \xi)^2], \quad (16)$$

where  $\lambda = (\Delta^2 + 2D_1 t)^{1/2}$ ,  $\beta = [4\rho_i^2 \sin^2(\omega_{ci} t/2)]$ , and  $B = (2\beta)^{1/2}/(2\pi\lambda)$ . Rearranging the terms and completing the integral over  $d\xi$  results in a Gaussian density distribution in space:

$$n_D(x, t) = B(2\pi)^{1/2} (\lambda^{-2} + \beta)^{-1/2} \times \exp[-x^2/(\beta^{-1} + 2\lambda^2)]. \quad (17)$$

The full-width at half-maximum of this density distribution is

$$X_{FWHM}^2 = 2.77 [4\rho_i^2 \sin^2(\omega_{ci} t/2) + 2\Delta^2 + 4D_1 t], \quad (18)$$

where  $\rho_i (\equiv v_1/\omega_{ci})$  is the Larmor radius.

If the tag beam and the detection optics are separated axially by  $\Delta z$ , then the time  $t$  is associated with a separation  $\Delta z = v_d t$  because of the axial plasma drift  $v_d$ . From the  $\sin^2(\omega_{ci} t/2)$  term, a spatial and temporal oscillation in the width is expected, resulting from the plasma's axial drift. However, the thermal spread of the axial velocities will cause particles that started in phase at the tag point to become out of phase later, effectively smearing the oscillation. Calculations indicate full decorrelation after drifting about 1.6 cm axially. Thus on experimental scales, the oscillations are

averaged out. The full-width at half-maximum becomes

$$X_{FWHM}^2 \cong 2.77(2\rho_i^2 + 2\Delta^2 + 4D_1 t). \quad (19)$$

Since for this experiment  $\rho_i$  and  $\Delta$  are independent of the axial drift, the change in  $X_{FWHM}^2$  between two different axial separations  $z_1$  and  $z_2$  is given by

$$\begin{aligned} \Delta X_{FWHM}^2 &= X_{FWHM}^2(z_1) - X_{FWHM}^2(z_2) \\ &\cong 2.7 [4D_1 (t_1 - t_2)] \\ &\cong 2.77 [4D_1 (z_1 - z_2)/v_d]. \end{aligned} \quad (20)$$

By measuring the  $\Delta X_{FWHM}^2$  as a function of various parameters the properties of the diffusion coefficient  $D_1$  can be determined.

A typical radial density profile is shown in Fig. 3. The plasma radius was 2.5 cm, but all tagged particle measurements were made within  $r \leq 0.5$  cm. Over the spatial range of the measurements the total density changed by 5%, corresponding to  $L_n \equiv (\nabla n/n)^{-1} \approx 15.6$  cm. Radial temperature profiles showed similar scale lengths. Typical scales for the tagged population gradient are of order of the Larmor radius (two orders of magnitude less than  $L_n$ ). Hence contributions to tagged particle diffusion resulting from gradients in the total density or temperature were negligible.

The density fluctuation level in the plasma was measured using a probe with a cylindrical tip of radius  $6.35 \times 10^{-3}$  cm and length  $2 \times 10^{-1}$  cm, the axis of the tip being oriented parallel to  $\mathbf{B}_0$ . Fluctuations were examined for frequencies less than 200 MHz. The radial profile of the fluctuation level is displayed in Fig. 4. The dominant region of fluctuations is the outermost edge of the plasma, well away from the region of tagged particle measurements. These plasma oscillations have characteristic frequencies in the very low kilohertz range and may be attributed to drift waves<sup>18</sup> at the plasma edge, where substantial temperature and density gradients could drive the waves. In the region where the tagged particle measurements were made, the density fluctuation level was less than  $2 \times 10^{-3}$ . For collisional diffusion to be dominant over turbulent contributions theory<sup>44</sup> predicts the fluctuation level should be less than 1%. Thus collisional diffusion was expected to be the dominant diffusive mechanism for test ions in this plasma.

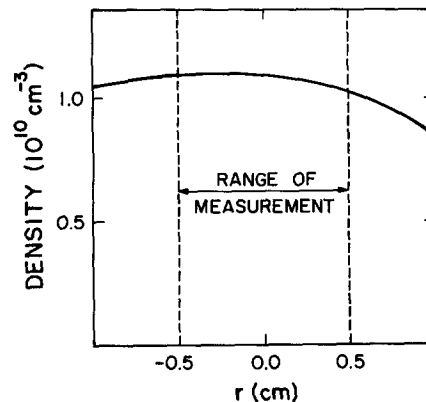


FIG. 3. Radial plasma density profile ( $n \approx 1.1 \times 10^{10} \text{ cm}^{-3}$ ,  $B_0 = 3 \text{ kG}$ ) showing a 5% change in density over the spatial range of measurement.

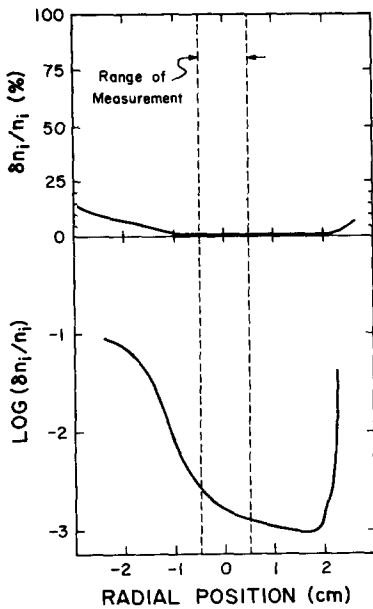


FIG. 4. Radial ion density fluctuation profile showing  $\delta n/n < 0.002$  over most of the spatial range of measurement ( $r < 0.5$  cm).

An example of the measured tagged particle radial profile at two different axial locations is given in Fig. 5. The radial profiles are taken by scanning the detection beam and collection optics in the  $x$  direction, as shown in the subfigures of Fig. 1. Comparison of the full-widths at half-maximum shows the diffusive radial spreading of the test ions as they travel axially (in Fig. 5 the two detection beam scans are separated axially by 18 cm). Equation (20) then gives  $D_{\perp}$  when  $v_d$  is known. For the condition of this experiment  $v_d \approx 7 \times 10^4$  cm/sec (see Refs. 38 and 43 for how this may be measured).

Plasma rotation must be considered since it would lead to an apparent spread in the  $x$ -direction test ion profile as a result of the laser beam geometry. A radial electric field will cause an azimuthal drift of  $v_{\theta} = cE_r/B_z$ . Because the laser

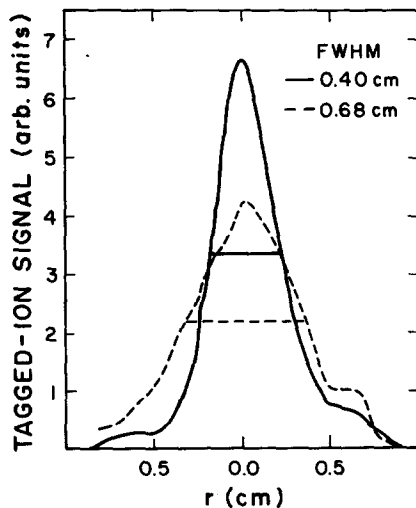


FIG. 5. Horizontal radial tagged particle profiles at two axial positions (separated by  $\delta z = 18$  cm) displaying radial spreading of test particles resulting from diffusion as plasma drifts down the magnetic field.

tags a vertical column of ions, the horizontal spreading of the tagged profile will be enhanced by  $(\cos \theta)^{-1}$ , where  $\theta$  is the angle of plasma rotation that occurs between ion tagging and detection. Measurements similar to the technique used by Wickham<sup>45</sup> showed radial electric fields of order  $3 \times 10^{-2}$  V/cm, giving a maximum rotation of  $\dot{\theta} \lesssim 3.6 \times 10^2$  rad/sec. Over the axial range of the test ion profile this leads to an apparent broadening of the test ion profile by 0.5% or an overestimate of diffusion by about 1%. Hence plasma rotation effects may be ignored for this experiment.

The test ion classical diffusion coefficient estimated by Eq. (5) goes as  $n/B^2$ . In contrast to this, anomalous diffusion coefficients (such as those predicted by Bohm<sup>46</sup> and Dupree<sup>44</sup>) generally are independent of density. Figure 6 shows the experimentally inferred values of  $D_{\perp}$  over the range of densities tested. The shaded areas are the theoretical predictions of Eq. (5), Bohm, and Dupree ( $D_{ii}$ ,  $D_B$ , and  $D_T$ , respectively), using measured values of  $n$ ,  $\langle (\delta n/n_0)^2 \rangle^{1/2}$ ,  $B$ , and  $T$  (including error bars), and are not fit to the data. Two conclusions may be drawn from this figure. First, the experimentally inferred  $D_{\perp}$  has a linear density dependence. Second, the magnitude of the inferred  $D_{\perp}$  is in agreement with classical test ion diffusion predictions.

The magnetic field was varied over a range of 2.25 to 6 kG while holding the density constant. The resulting inferred diffusion coefficients are displayed in Fig. 7. It is possible to fit  $1/B^2$  and  $1/B$  curves through the error bars of the data, so these data do not establish the magnetic field dependence conclusively. One may say that the inferred test ion diffusion coefficient has a magnetic field dependence near  $1/B^2$ , but a stronger statement about field dependence should not be made based on these data. Using the measured  $n$ ,  $B$ , and  $T$  values (including error bars) one may calculate  $D_{\perp}$  from Eq. (5). This calculation is plotted in Fig. 7 as the shaded area labeled  $D_{ii}$ . Also using the measured plasma properties allows predictions for Bohm diffusion<sup>46</sup> and turbulent diffusion,<sup>44</sup> labeled  $D_B$  and  $D_T$ , respectively, on Fig. 7. The experimentally inferred  $D_{\perp}$  agrees, within the error bars, with the classical prediction. There is an order of mag-

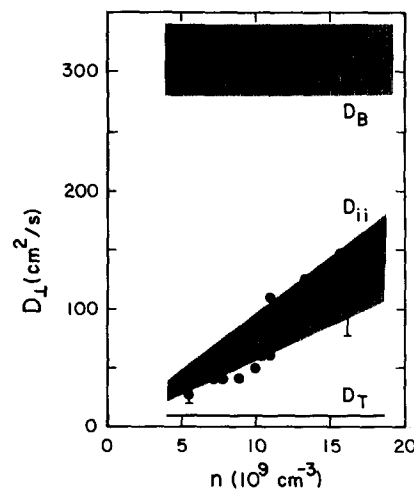


FIG. 6. Measured test ion diffusion coefficient versus density in a quiet plasma. Shaded areas are theoretical predictions for Bohm ( $D_B$ ), collisional ( $D_{ii}$ ), and turbulent ( $D_T$ ) diffusion.

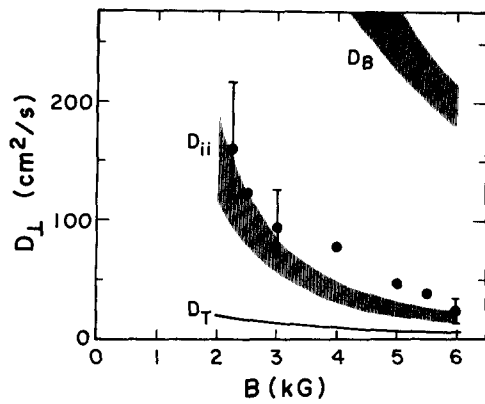


FIG. 7. Measured test ion diffusion coefficient versus the magnetic field in a quiet plasma. Shaded areas are theoretical predictions for Bohm ( $D_B$ ), collisional ( $D_{ii}$ ), and turbulent ( $D_T$ ) diffusion.

nitude disagreement with Bohm diffusion and a factor of 6 disagreement with the turbulent diffusion prediction. The data are consistent with diffusion dominated by classical collisions with a small addition as a result of low level of turbulence.

The experiments reported here measured test ion transport when  $\langle(\delta n/n_0)^2\rangle^{1/2}$  was of the order of  $2 \times 10^{-3}$  or less, which we have characterized as a quiet plasma. Thus far we also have been able to use this dark-pulse tagging method to examine ion transport for turbulent conditions with  $\langle(\delta n/n_0)^2\rangle^{1/2}$  up to  $5 \times 10^{-2}$ . Preliminary results were reported previously<sup>20</sup> and more detailed experiments have been performed. These results are outside the scope of the present paper, since the plasma can no longer be characterized as quiet, and will be reported in the future.

#### IV. CONCLUSIONS

Measurements were made of the cross-field transport of test ions in a quiet plasma. The modified Langevin equation predicts a cross-field diffusion coefficient of  $D_{\perp} = \frac{1}{2} \rho_i^2 \nu_{ii}$  for test ions in a quiet plasma. The experimental results agree with the predictions of the modified Langevin equation, Rostoker,<sup>1</sup> and Klimontovich.<sup>28</sup> The experimental results disagree with predictions of anomalous diffusion for these plasma parameters.

#### ACKNOWLEDGMENTS

We would like to thank Dr. J. Krommes, Dr. N. Rynn, Dr. R. Stern, Dr. W. Thompson, and Dr. R. Walkup for discussions. Mr. Stacy Roe provided helpful laboratory support.

- <sup>1</sup>N. Rostoker, Nucl. Fusion **1**, 101 (1960).
- <sup>2</sup>N. Rostoker and M. N. Rosenbluth, Phys. Fluids, **3**, 1 (1960).
- <sup>3</sup>N. Rostoker, Phys. Fluids **7**, 479 (1964).
- <sup>4</sup>N. Rostoker, Phys. Fluids **7**, 491 (1964).
- <sup>5</sup>N. D'Angelo and N. Rynn, Phys. Fluids **4**, 275 (1961).
- <sup>6</sup>N. D'Angelo and N. Rynn, Phys. Fluids **4**, 1303 (1961).
- <sup>7</sup>W. Stodiek, R. A. Ellis, Jr., and J. G. Gorman, Nucl. Fusion Suppl. Part 1, 193 (1962).
- <sup>8</sup>N. Rynn, Phys. Fluids **7**, 1084 (1964).
- <sup>9</sup>N. D'Angelo, Phys. Fluids **7**, 1086 (1964).
- <sup>10</sup>N. D'Angelo and S. von Goeler, Nucl. Fusion **5**, 279 (1965).
- <sup>11</sup>R. W. Motley, Phys. Fluids **8**, 205 (1965).
- <sup>12</sup>N. S. Wolf and K. C. Rogers, Phys. Fluids **9**, 2294 (1966).
- <sup>13</sup>S. von Goeler and R. W. Motley, Phys. Fluids **10**, 1360 (1967).
- <sup>14</sup>S. von Goeler, M. Sadowski, H. Pacher, and S. Yoshikawa, Phys. Fluids **13**, 790 (1970).
- <sup>15</sup>E. Guilino, Phys. Fluids **13**, 1855 (1970).
- <sup>16</sup>B. Eastlund, Phys. Fluids **9**, 594 (1966).
- <sup>17</sup>R. L. Stenzel and W. Gekelman, Phys. Fluids **21**, 2024 (1978).
- <sup>18</sup>H. W. Hendel, T. K. Chu, and P. A. Politzer, Phys. Fluids **11**, 2426 (1968).
- <sup>19</sup>R. A. Stern, D. N. Hill, and N. Rynn, Phys. Lett. A **93**, 127 (1983).
- <sup>20</sup>R. McWilliams, D. N. Hill, N. S. Wolf, and N. Rynn, Phys. Rev. Lett. **50**, 836 (1983).
- <sup>21</sup>S. M. Kaye, R. J. Goldston, M. Bell, K. Bol, M. Bitter, R. Fonck, B. Grek, R. J. Hawryluk, D. Johnson, R. Kaita, H. Kugel, D. Mansfield, D. McCune, K. McGuide, D. Mueller, M. Okabayashi, D. Owens, G. Schmidt, and P. Thomas, Nucl. Fusion **24**, 1303 (1984).
- <sup>22</sup>E. S. Marmor, J. E. Rice, J. L. Terry, and F. H. Seguin, Nucl. Fusion **22**, 1567 (1982).
- <sup>23</sup>F. L. Hinton and R. D. Hazeltine, Rev. Mod. Phys. **48**, 239 (1976).
- <sup>24</sup>P. C. Liewer, Nucl. Fusion **25**, 543 (1985).
- <sup>25</sup>S. Chandrasekhar, Rev. Mod. Phys. **15**, 1 (1943).
- <sup>26</sup>W. Thompson and J. Hubbard, Rev. Mod. Phys. **32**, 714 (1960).
- <sup>27</sup>M. Kac, Am. Math. Mon. **54**, 369 (1947).
- <sup>28</sup>Yu. L. Klimontovich, *The Statistical Theory of Non-Equilibrium Processes in a Plasma* (MIT, Cambridge, MA, 1967).
- <sup>29</sup>A. Simon, Phys. Rev. **100**, 1557 (1955).
- <sup>30</sup>C. L. Longmire and M. N. Rosenbluth, Phys. Rev. **103**, 507 (1956).
- <sup>31</sup>J. B. Taylor, Phys. Fluids **4**, 1142 (1961).
- <sup>32</sup>N. Rynn, Rev. Sci. Instrum. **35**, 40 (1964).
- <sup>33</sup>P. M. Bellan and M. Porkolab, Phys. Fluids **19**, 995 (1976).
- <sup>34</sup>R. M. Measures, J. Appl. Phys. **39**, 5232 (1968).
- <sup>35</sup>D. Dimock, E. Hinnov, and L. C. Johnson, Phys. Fluids **12**, 1730 (1969).
- <sup>36</sup>R. A. Stern and J. A. Johnson, Phys. Rev. Lett. **34**, 1548 (1975).
- <sup>37</sup>R. A. Stern, D. N. Hill, and N. Rynn, Phys. Rev. Lett. **47**, 792 (1981).
- <sup>38</sup>D. N. Hill, S. Fornaca, and M. G. Wickham, Rev. Sci. Instrum. **54**, 309 (1983).
- <sup>39</sup>A. Gallagher, Phys. Rev. **157**, 24 (1967).
- <sup>40</sup>P. G. Pappas, M. M. Burns, D. D. Hinshelwood, and M. S. Feld, Phys. Rev. A **21**, 1955 (1980).
- <sup>41</sup>R. A. Stern, Phys. Fluids **21**, 1287 (1978).
- <sup>42</sup>D. N. Hill, Ph.D. thesis, University of California, Irvine, 1983, p. 87.
- <sup>43</sup>R. McWilliams and R. Koslover, Phys. Rev. Lett. **58**, 37 (1987).
- <sup>44</sup>T. H. Dupree, Phys. Fluids **10**, 1049 (1967).
- <sup>45</sup>M. Wickham, Ph.D. thesis, University of California, Irvine, 1981.
- <sup>46</sup>D. Bohm, in *The Characteristics of Electrical Discharges in Magnetic Fields*, edited by A. Guthrie and R. K. Wakerling (McGraw-Hill, New York, 1949), p. 77.